Published in final edited form as:
J Mol Cell Cardiol. 2010 October ; 49(4): 617–624. doi:10.1016/j.yjmcc.2010.07.011.

Role of CaMKII in RyR Leak, EC Coupling and Action Potential Duration: A Computational Model

Yasmin L. Hashambhoy, **Joseph L. Greenstein**, and **Raimond L. Winslow**
Institute for Computational Medicine, Center for Cardiovascular Bioinformatics and Modeling, and the Whitaker Biomedical Engineering Institute, The Johns Hopkins University, Baltimore, MD, USA

Abstract

During heart failure, the ability of the sarcoplasmic reticulum (SR) to store Ca^{2+} is severely impaired resulting in abnormal Ca^{2+} cycling and excitation-contraction (EC) coupling. Recently, it has been proposed that "leaky" ryanodine receptors (RyRs) contribute to diminished Ca^{2+} levels in the SR. Various groups have experimentally investigated the effects of RyR phosphorylation mediated by Ca^{2+}/calmodulin-dependent kinase II (CaMKII) on RyR behavior. Some of these results are difficult to interpret since RyR gating is modulated by many external proteins and ions, including Ca^{2+}. Here, we present a mathematical model representing CaMKII-RyR interaction in the canine ventricular myocyte. This is an extension of our previous model which characterized CaMKII phosphorylation of L-type Ca^{2+} channels (LCCs) in the cardiac dyad. In this model, it is assumed that upon phosphorylation, RyR Ca^{2+}-sensitivity is increased. Individual RyR phosphorylation is modeled as a function of dyadic CaMKII activity, which is modulated by local Ca^{2+} levels. The model is constrained by experimental measurements of Ca^{2+} spark frequency and steady state RyR phosphorylation. It replicates steady state RyR (leak) fluxes in the range measured in experiments without the addition of a separate passive leak pathway. Simulation results suggest that under physiological conditions, CaMKII phosphorylation of LCCs ultimately has a greater effect on RyR flux as compared with RyR phosphorylation. We also show that phosphorylation of LCCs decreases EC coupling gain significantly and increases action potential duration. These results suggest that LCC phosphorylation sites may be a more effective target than RyR sites in modulating diastolic RyR flux.

Keywords

CaMKII; RyR; EC coupling; L-type Ca channel; computational model

Introduction

During heart failure (HF), cardiac Ca^{2+} cycling is disturbed, resulting in altered excitation-contraction coupling (ECC). One of the causes of this disruption is a diminished sarcoplasmic reticulum (SR) Ca^{2+} uptake rate, which hinders the ability of the SR to store adequate levels of Ca^{2+} [1,2]. Additionally, it has been suggested that during HF, Ca^{2+} leak via ryanodine

Address Correspondence to: Raimond L. Winslow, PhD, Rm 315 CSEB., 3400 N. Charles St., Baltimore MD 21218, 410.516.5417 (Office), 410.516.5294 (FAX), rwinslow@jhu.edu.

receptors (RyRs) increases, further limiting SR Ca^{2+} (Ca_{SR}) load [3–5]. The existence and cause of this RyR leak has been debated extensively, however there is growing evidence pointing to a critically important role of localized kinases, such as Ca^{2+}/calmodulin-dependent kinase II (CaMKII) [3,6] in the modulation of RyR function.

CaMKII activity is dynamically regulated by Ca^{2+}, calmodulin (CaM) and phosphatases. It targets a number of proteins involves in ion transport in the cardiac ventricular myocyte, including L-type Ca^{2+} channels (LCCs), phospholamban (PLB) and RyRs. The large number of potential ECC-related CaMKII targets makes it difficult to quantify how phosphorylation of each target contributes to the integrative properties of ECC and myocyte function. This has motivated the development of a number of computational models of CaMKII action [7–10]. This study presents a novel computational model which incorporates the interaction of CaMKII with its major ECC targets: LCCs, RyRs and PLB. It builds upon our previous model which describes dynamic CaMKII phosphorylation of LCCs [8] and L-type Ca^{2+} current (I_{CaL}) facilitation. The goal of this study is to use model simulations to answer the following question: how does differential CaMKII phosphorylation of LCCs, RyRs and PLB modulate RyR Ca^{2+} flux (leak), ECC and action potential (AP) duration?

Modeling the direct interaction between CaMKII and RyRs poses a challenge since there are many conflicting experimental results regarding CaMKII-mediated changes in RyR behavior. RyR open probability (P_o) has been shown to increase [11–13] or decrease [14,15] in the presence of CaMKII. These inconsistencies may be due to variations in methods of RyR isolation and preparation. In addition, the high sensitivity of RyR gating to cytosolic Ca^{2+} concentration ($[Ca_{cyt}]$) and $[Ca_{SR}]$ makes it difficult to interpret experiments in which $[Ca_{cyt}]$ and $[Ca_{SR}]$ are not tightly controlled. Recently, Guo et al [12] used an experimental protocol in which $[Ca_{cyt}]$ and $[Ca_{SR}]$ were tightly controlled to show that CaMKII phosphorylation of RyRs increases P_o. Their Ca^{2+} spark frequency (CaSpF) measurements in the absence and presence of CaMKII, in conjunction with results from CaMKII phosphorylation assays, are used to constrain parameters of this new model. Additionally, CaMKII-mediated phosphorylation of PLB and the subsequent dis-inhibition of the SR Ca^{2+} pump (SERCA) is modeled. This mechanism, in turn, regulates $[Ca_{SR}]$ and RyR gating.

The model presented in this study is unique in that it simulates independent individual dyadic Ca^{2+} compartments and determines the state of local Ca^{2+} dependent processes such as CaMKII activity, RyR activation and LCC inactivation. Thus, simulations can be used to make predictions about whole-cell phenomena that are governed by the dynamics of local Ca^{2+}. The results show that LCC phosphorylation ultimately leads to increased diastolic RyR leak and action potential duration (APD), and that LCC and RyR phosphorylation have identifiably distinct effects on ECC.

Materials and Methods

The CaMKII-RyR computational model builds upon our previous work [8], which described CaMKII phosphorylation of LCCs, with model parameters carefully constrained by experimental data, in a stochastic, local control model of the canine cardiac ventricular myocyte [16]. It is assumed that a dodecameric CaMKII holoenzyme is tethered to each LCC, and that LCCs, RyRs and kinase monomers respond to dyadic Ca^{2+} levels ($[Ca_{dyad}]$). The model tracks individual LCCs, RyRs and CaMKII holoenzymes, as well as $[Ca_{dyad}]$ and the junctional $[Ca_{SR}]$ ($[Ca_{JSR}]$) associated with each dyadic space. CaMKII is activated when bound by Ca^{2+}/CaM, and/or phosphorylated at T287. The CaMKII model transitions between various conformational states, each of which is associated with a different bound and/or phosphorylated configuration (see Figure 2 in Hashambhoy et al [8]). Each state is associated with a

corresponding CaMKII activity coefficient, which represents the state's phosphorylation rate normalized to the maximum phosphorylation rate of CaMKII.

CaMKII phosphorylates LCCs and RyRs dynamically as a function of kinase activity. This dynamic phosphorylation captures the Ca^{2+} feedback between LCCs and RyRs (which allow Ca^{2+} to enter the dyad) and CaMKII (which is activated by Ca^{2+} and regulates LCC and RyR function), thus allowing for correlation between channel openings and phosphorylation.

LCC gating is modeled as described previously [8] with voltage- and Ca^{2+}-dependent rate parameters. When an LCC is fully phosphorylated by CaMKII, it transitions to a highly active mode of gating known as mode 2. Mode 2 channels exhibit a longer mean open time (resulting from a reduced transition rate out of the open state) compared to unphosphorylated channels which gate in mode 1, the normal mode of gating [17,18].

In the new model, CaMKII dynamically phosphorylates RyRs at a rate proportional to dyadic CaMKII activity. A modified version of the four state RyR model presented by Shannon et al [19] is incorporated into the local control myocyte model (see Figure 1).

The integrated Shannon model incorporates $[Ca_{dyad}]$- and $[Ca_{JSR}]$-dependent RyR inactivation and is able to reproduce Ca^{2+} spark properties (such as spark duration and Ca_{JSR} depletion, see DS "Model Validation"). In the original model, RyRs reside in one of four states: closed (R), open (O), inactivated (I), or closed and inactivated (RI). Transitions between these states are governed by $[Ca_{dyad}]$ as well as $[Ca_{JSR}]$. The model presented here is an eight-state model comprised of two mirrored groups of four state models, one representing unphosphorylated RyRs, and the other representing phosphorylated RyRs. Transitions to the phosphorylated states are governed by the dynamic rate of phosphorylation, which is dependent on dyadic CaMKII activity. Return to the unphosphorylated states is mediated by a constant rate of dephosphorylation.

Based on experimental results [20,21], it is assumed that CaMKII phosphorylation of RyRs leads to heightened Ca^{2+} sensitivity which results in increased RyR P_o. In the RyR model, this translates to increases in the R to O and RI to I kinetic rate constants (compare unphosphorylated and phosphorylated models in Fig. 1A). These rate constants are dependent on both $[Ca_{dyad}]$ and $[Ca_{JSR}]$. Maximal rate of CaMKII phosphorylation of RyRs is constrained by in vitro experimental results [11]. The rate of dephosphorylation is constrained such that under simulation of 0.1 Hz and 2 Hz pacing, RyR phosphorylation levels match those reported in experiments at RyR site S2815, which has been shown in experiments to be a CaMKII specific site [22].

Transition rates in the phosphorylated RyR model are identical to those in the unphosphorylated model, except for the addition of a multiplicative factor Ca_{Shift} in the horizontal Ca^{2+}-dependent rates, which simulates an increase in Ca^{2+} sensitivity in the RyR opening rate and the rate from state RI to state I (in order to maintain macroscopic reversibility). In the Shannon et al RyR model [19], luminal Ca^{2+} modulates RyR affinity for $[Ca_{cyt}]$; thus an alteration in the sensitivity to luminal Ca^{2+} also alters RyR sensitivity to $[Ca_{cyt}]$ (and vice versa). Thus, altering either $[Ca_{dyad}]$ or $[Ca_{JSR}]$ sensitivity results in the same net effect of increased RyR sensitivity, and are therefore qualitatively indistinguishable in this model. A Nelder Mead Simplex algorithm (MATLAB, The Mathworks, Inc.) was used to calculate the optimal value for Ca_{Shift} that would result in a steady state RyR P_o increase matching the CaSpF augmentation reported by Guo et al [12] in wild type (WT) and PLB knockout (PLB-KO) myocytes. Ca_{Shift} was optimized to a value of 1.3, which yields steady state RyR P_o increases of 129% and 69% for the WT and PLB-KO cases, respectively (the data show 150% and 98% increases in CaSpF [12]).

The Ca^{2+} spark results in the "ECC Gain" section are derived from simulations performed 5 times at each membrane potential in each scenario. In each simulation, individual LCC and RyR fluxes were analyzed from 250 functional release units.

Additionally, the model describes cytosolic CaMKII phosphorylation of PLB. Binding of PLB to the SERCA pump has been shown to decrease SR Ca^{2+} uptake by reducing the affinity of the pump for Ca^{2+}. Phosphorylation of PLB relieves its inhibition of SERCA [23], and Ca^{2+} affinity returns to that in the PLB-unbound state. The PLB-SERCA model is a modified version of the SERCA pump model presented by Shannon et al [24]. Fractional PLB phosphorylation and dephosphorylation are described using Michaelis-Menten equations, where V_{max} and K_m are derived from in vitro experiments [25,26]. A full description of the complete model can be found in the Data Supplement (DS). One way ANOVA significance tests were used to calculate all p values and data are presented as mean ± S.E.M.

Results

CaSpF Simulation

The CaSpF protocols employed by Guo et al [12] were simulated in the stochastic model. In the presence of CaMKII, CaSpF is 54.34 sparks/pL/s. This is 168% higher than that CaSpF in the absence of CaMKII (20.26 sparks/pL/s). In the presence of CaMKII, Ca^{2+} sparks depleted Ca_{JSR} by 32% on average, which is in agreement with reported Ca^{2+} blink results [27] (data not shown). Simulation details, including plots of typical Ca^{2+} sparks, can be found in the DS.

SR Leak

"SR Ca^{2+} leak" is defined as loss of Ca^{2+} from the SR under resting conditions [28]. The mechanisms involved in SR Ca^{2+} leak remain unclear, and this poses a challenge in formulating a mathematical model that describes the relevant leak mechanism(s). Shannon et al [19] introduced a passive SR Ca^{2+} leak pathway to their common pool myocyte model in order to match experimentally observed diastolic leak.

This model achieves experimentally measured levels of SR Ca^{2+} leak in the absence of a separate passive leak. The SR leak measurement protocol employed by Shannon et al [29] was simulated in the absence of external Na^+ and Ca^{2+}. At a free $[Ca_{SR}]$ level of 0.7 mmol/L SR, the model SR Ca^{2+} leak is 4.8 μmol/L cytosol/s. These results are in good agreement with Shannon et al [29], who reported a value of 5 μmol/L cytosol/sec at this SR load.

Effects of LCC and RyR Phosphorylation on ECC Gain

ECC gain is defined as the ratio of peak RyR flux to peak LCC flux [30] and varies with membrane potential. Figure 2 shows ECC simulations performed in the presence or absence of CaMKII-mediated phosphorylation of LCCs and/or RyRs. Measurement of ECC gain is preceded by voltage clamp pacing, to activate CaMKII. Since pacing loads the SR and affects Ca_{cyt} levels (Figure 2A and 2C), gain simulations were repeated with initial $[Ca_{SR}]$ and $[Ca_{cyt}]$ reset to matched values ($[Ca_{SR}]$=0.75 mM and $[Ca_{cyt}]$=75 nM) in order to isolate the changes in ECC gain that could be attributed to altered kinetics of the phosphorylated channels (Figure 2B and 2D). Panels A and B of Figure 2 show ECC gain curves, in the absence of LCC phosphorylation, in which the maximum RyR phosphorylation rate was varied in order to control the fraction of phosphorylated RyRs. Since this is a stochastic model, multiple simulations were performed at each test voltage. Figure 2A shows that increased RyR phosphorylation (black line) results in an increase in ECC gain. Figure 2B demonstrates an even greater effect of RyR phosphorylation on ECC gain. The smaller change in gain in Figure 2A as compared to Figure 2B results from the compensatory reduction in Ca_{SR} that occurs during the preceding pacing protocol in response to increased RyR activity (data not shown).

In both cases, the increase in gain with RyR phosphorylation is more pronounced at depolarized potentials, where LCC unitary current is relatively small, and the phosphorylation-mediated increase in RyR Ca^{2+} sensitivity improves the fidelity of local coupling between LCCs and RyRs. The observed relationship between ECC gain and the extent of RyR phosphorylation is consistent with the change in the number of Ca^{2+} sparks underlying the SR release flux. For all simulations, sparks were counted over a 32 ms time window centered at the time of peak RyR flux. For the protocol of Figure 2B, there is a modest increase in CaSpF with increased RyR phosphorylation at hyperpolarized potentials (4416 vs. 3750 sparks/pL/s at −30 mV depolarization, $p<0.01$). The prominent increase in gain at depolarized potentials is consistent with a greater number of Ca^{2+} sparks (3076 vs. 2311 sparks/pL/s at +50 mV depolarization, $p<0.01$), and a greater SR release flux without an increase in I_{CaL} (as shown in DS Figure DS2). While the increase in the number of sparks is a major driving force behind the observed increases in ECC gain, RyR phosphorylation also causes an increase in RyR recruitment (see Figure DS3 for a full analysis). In the model, phosphorylation increases RyR Ca^{2+} sensitivity, therefore increased RyR recruitment is expected and is consistent with the increases in spark duration observed by Guo et al[12].

A very different shift in the ECC gain curve results from varying the degree of LCC phosphorylation in the absence of RyR phosphorylation, as is shown in panels C and D of Figure 2. At hyperpolarized potentials, LCC phosphorylation results in larger I_{CaL} (as demonstrated previously [8]), but with minimally enhanced Ca^{2+} release, which translates to reduced ECC gain. Similar changes in gain are predicted with (panel C) and without (panel D) matched values of $[Ca_{SR}]$ and $[Ca_{cyt}]$. In panel D, the increase in ECC gain with 6.4% LCC phosphorylation compared to that with 0.6% phosphorylation at depolarized potentials arises from augmented Ca_{cyt} and SR Ca^{2+} loading. While LCC phosphorylation increases LCC P_o, it does so by prolonging open duration. At hyperpolarized potentials, unitary I_{CaL} is relatively high, therefore RyR recruitment already occurs with high fidelity and is therefore affected minimally by LCC phosphorylation (see DS Figure DS2). At −30 mV, for the protocol of Figure 2D, increased vs. decreased LCC phosphorylation results in no significant difference in CaSpF (3873 sparks/pL/s) or the number of RyRs recruited per spark. However, peak I_{CaL} is ~50% higher in the 6.4% LCC phosphorylation case compared to 0.6% LCC phosphorylation (see DS Figure DS2D), therefore the net result of increased LCC phosphorylation is decreased ECC gain. At depolarized potentials, the increased LCC phosphorylation does not significantly affect the CaSpF (2155 sparks/pL/s at +50 mV) or RyR recruitment, and there is no significant difference in ECC gain (Figure 2D) because of the very small increase in I_{CaL} (see DS Figure DS2F). Over the full range of potentials, the ECC gain curve becomes more shallow with increased LCC phosphorylation due to the dominant effect of increased I_{CaL} resulting from mode 2 LCC gating.

Effect of LCC and RyR Phosphorylation on Action Potential

Figure 3A displays the effects of LCC and RyR phosphorylation on APD. “LCC and RyR Phosphorylation” refers to the case in which both LCCs and RyRs are dynamically phosphorylated by CaMKII activity; “LCC Phosphorylation Only” is the case where LCCs are dynamically phosphorylated and RyRs cannot be phosphorylated; “RyR Phosphorylation Only” is the case where RyRs are dynamically phosphorylated and LCCs cannot be phosphorylated; “No Phosphorylation” means that neither LCCs nor RyRs are phosphorylated. The average APD at 90% repolarization (APD_{90}) over 50 beats is significantly larger with LCC phosphorylation (compare the LCC Phosphorylation Only (374 ms) and LCC and RyR Phosphorylation (380 ms) cases with RyR Phosphorylation Only (296 ms) and No Phosphorylation (281 ms) cases). Even though there is only a modest difference in peak I_{CaL} due to LCC phosphorylation, there is a significant increase in sustained I_{CaL}. LCC phosphorylation increases the number of channels operating in mode 2 gating [8] which results

in increased I_{CaL} during the plateau phase of the AP (compare the grey and black lines in Figure 3B). This results in increased APD. Physiological levels of RyR phosphorylation have no significant effects on APD.

Effect of LCC and RyR Phosphorylation on Ca^{2+} Dynamics during AP Pacing

Figure 4 presents Ca^{2+} cycling properties underlying APs at 1 Hz pacing. Figure 4A shows $[Ca_{SR}]$. Prior to application of the stimulus current, $[Ca_{SR}]$ is ~0.72 mM. I_{CaL} triggers RyR openings and Ca^{2+} release from junctional SR (JSR). Figure 4B shows $[Ca_{cyt}]$. At the beginning of the pulse, RyR flux (Figure 4C) is greater than SERCA flux (Figure 4D) and $[Ca_{SR}]$ depletes to ~0.43 mM. Subsequently, SERCA flux dominates and SR refills to its prestimulus level. From Fig. 4A, it is clear that in the presence of LCC phosphorylation, $[Ca_{SR}]$ is elevated (compare the solid black line to the dark grey line). It is not immediately apparent whether the shifts in $[Ca_{SR}]$ are due to changes in a) SR Ca^{2+} uptake via SERCA, b) RyR behavior in response to trigger I_{CaL}, or c) RyR leak. The effects of these factors will be addressed in order.

Since LCC phosphorylation results in mode 2 gating, the apparent rate of inactivation of I_{CaL} decreases (as discussed in a previous study [8]) which results in an increase in Ca^{2+} flux into the cell, and the observed augmentation of peak Ca^{2+} transient (see Figure 4B). Additionally, LCC phosphorylation results in large increases in sustained I_{CaL} (which contributes to increases in APD as well as increases in Ca_{cyt}, and Ca_{SR}.). Figure 4D shows that Ca^{2+} flux into the SR is increased with LCC phosphorylation (dotted and solid black lines). This increase in Ca_{2+} flux is sensible, since $[Ca_{cyt}]$ is significantly increased in the presence of LCC phosphorylation (see Figure 4B), and the rate of SR Ca^{2+} uptake increases with $[Ca_{cyt}]$. $[Ca_{SR}]$ is increased by augmented SERCA function when LCCs are phosphorylated.

Figure 4E shows the diastolic RyR leak under various conditions. For the purpose of this study, diastolic leak is defined as the RyR flux during the second half of each pacing cycle. LCC P_o was measured for every AP in each 1Hz pacing simulation. In every case, there are 0 LCCs open during the 500 – 1000 ms time period after initial stimulus. Thus, diastolic leak (as defined in this study) occurs in the absence of trigger I_{CaL}.

In the absence of any phosphorylation, diastolic RyR leak averages 6.8 μmol/L/s (dark grey line). In the presence of RyR phosphorylation only, diastolic leak increases significantly to 9.7 μmol/L/s (light grey line). However, in the presence of LCC phosphorylation alone, RyR leak increases to a much greater extent, to 24.9 μmol/L/s (black line). LCC and RyR phosphorylation results in an average leak of 28.2 μmol/L/s (dotted black line).

These results show that SR leak via RyRs is affected to a greater extent by the indirect consequences of CaMKII-mediated LCC phosphorylation than by RyR phosphorylation. Even when all RyRs are phosphorylated, diastolic RyR leak does not significantly increase above 11 μmol/L/s in the absence of LCC phosphorylation (data not shown). To further illustrate the effect of LCC phosphorylation on RyR leak, additional simulations were performed in which the fraction of phosphorylated LCCs was varied (see Figure 4F). Diastolic RyR leak rises significantly as the fraction of LCCs gating in mode 2 increases.

Further analysis on Ca^{2+} transients revealed that in the absence of LCC phosphorylation, when the RyR phosphorylation rate was increased by 50%, Ca^{2+} transients decreased significantly ($p<0.05$) from a peak of 710 nM to 694 nM. This corresponded to change in leak from 6.8 μM/s to 9.59 μM/s diastolic leak. At 100% RyR phosphorylation, the average Ca^{2+} transient reached a peak of 646 nM, approximately 10% decrease from the case in which there was no RyR phosphorylation. These small changes in leak occur, in part, as a result of decreases in SR Ca^{2+} load that accompany increased RyR phosphorylation.

Mechanisms of RyR Leak

Results from Figure 4 show that LCC phosphorylation leads to a notable increase in RyR diastolic leak (compare the black and dark grey lines in Fig. 4E), however these data alone do not reveal the mechanisms altering leak. To isolate the influence of individual factors on RyR behavior, steady state RyR flux is calculated analytically as a function of $[Ca_{cyt}]$ and $[Ca_{JSR}]$ (see DS Figure DS4 for surface plots of RyR flux.) An analysis of the directional derivatives of RyR flux with respect to $[Ca_{cyt}]$ and $[Ca_{JSR}]$ demonstrates that RyR flux is far more sensitive to $[Ca_{cyt}]$ than to $[Ca_{JSR}]$. Thus, the LCC phosphorylation mediated increase in diastolic RyR leak can be attributed to the augmented $[Ca_{cyt}]$ resulting from mode 2 LCC gating.

Action Potentials Under Abnormal Conditions

Experiments have shown that during HF, CaMKII levels are elevated [3,31,32] and RyR-bound phosphatase levels are reduced [3,4]. Simulations were performed to isolate the effect of increased CaMKII phosphorylation of LCCs on APD by increasing the maximum rate of LCC phosphorylation. APD increases with enhanced fractional LCC phosphorylation (see Figure 3C). In addition, increased levels of LCC phosphorylation lead to generation of early-after depolarizations (EADs), in agreement with the results of Tanskanen et al [33], who found that EAD frequency increased with fractional mode 2 gating. Figure 5 illustrates an example of simulated EADs under elevated levels of LCC phosphorylation (4.8%), as may occur during CaMKII overexpression.

PLB Phosphorylation

Simulation results show that under normal physiological conditions at 1 Hz pacing, the fraction of PLB phosphorylated by CaMKII is minimal (~0.5%, data not shown) and has no significant effect on RyR leak or APD. This fractional phosphorylation is consistent with experimental approximations, which estimate that PLB phosphorylation is less than 5% at 2 Hz pacing [22].

Discussion

This study investigates how dynamic phosphorylation of three CaMKII targets, LCCs, RyRs, and PLB, affects SR Ca^{2+} leak and APD. The model is constrained by the results of various biochemical and Ca^{2+} spark frequency experiments. It is unique in that it describes the behavior of individual LCCs and RyRs responding to local CaMKII activity and $[Ca_{dyad}]$. Simulation results are able to replicate increases in Ca^{2+} spark frequency and RyR leak values that are in good agreement with those measured experimentally.

How is SR Ca^{2+} Leak Affected by LCC and RyR Phosphorylation?

Simulations show that RyR phosphorylation alone leads to decreased $[Ca_{SR}]$ and unchanged $[Ca_{cyt}]$ (compare the dark grey and light grey lines in Figs. 4A and 4B). This result is not surprising when one considers findings from caffeine experiments. Exposure to caffeine results in increased RyR sensitivity to Ca^{2+}, the same response assumed to be induced by CaMKII phosphorylation. In experiments on rat cardiac myocytes, Trafford et al [34] observed that low level caffeine application resulted in transient increases in systolic Ca^{2+}, which increased $[Ca_{cyt}]$ and increased the amount of Ca^{2+} pumped out of the cell through NCX, thus reducing $[Ca_{SR}]$. By solely increasing RyR Ca^{2+}-sensitivity, they found that they were unable to induce sustained alterations in the systolic Ca^{2+} transient. Their findings are mirrored by our simulation results, which show that phosphorylation of RyRs does not have a large sustained response on the systolic Ca^{2+} transient (see Fig. 4C).

The results from this study suggest that CaMKII phosphorylation of LCCs has a much larger effect on SR Ca^{2+} leak than phosphorylation of RyRs during pacing (Fig. 4). This finding has significant implications. Currently, there is debate regarding how CaMKII phosphorylation of RyR affects receptor function. Our simulation results suggest that even if RyR phosphorylation increases Ca^{2+} spark frequency in quiescent myocytes, the effect on diastolic SR Ca^{2+} leak is minimal compared to the effects resulting from LCC phosphorylation.

Phosphorylation and HF

Many groups have found that RyRs are hyper-phosphorylated during HF, and have suggested that block of RyR phosphorylation may reduce SR Ca^{2+} leak [3,4,35] This hypothesis is attractive, however SR Ca^{2+} leak studies are primarily based on RyR P_o experiments in lipid bilayers and Ca_{SR} leak measurements under controlled $[Ca_{cyt}]$ and $[Ca_{SR}]$ conditions. Our results predict that under physiological conditions, reducing CaMKII phosphorylation of LCCs may be a more effective approach to decreasing diastolic SR Ca^{2+} leak than reducing CaMKII phosphorylation of RyRs.

Many studies have linked CaMKII to arrhythmogenesis. Anderson et al. [36] demonstrated that inhibition of CaMKII activity significantly decreased likelihood of EADs in rabbit hearts and Sag et al showed that CaMKII inhibition reduces cardiac arrhythmogenesis [37]. While the cause of this behavior is unknown, our study suggests that RyR phosphorylation is not the culprit. In simulations, even the phosphorylation of all RyRs does not result in EAD generation (data not shown). This prediction confirms the findings of Venetucci et al [38] who were unable to produce arrhythmogenic behavior by increasing RyR P_o alone. However, we were able to reproduce EADs by hyper-phosphorylating LCCs (see Fig. 5), corroborating the modeling findings of Tanskanen et al [33], who showed that EADs can result from the clustered gating of LCCs in mode 2. This suggests that reduced likelihood of EAD generation on inhibition of CaMKII may be related to a reduction in LCC mode 2 gating rather than to effects on RyRs.

EC Coupling Gain

Experimental studies have shown that at hyperpolarized potentials, ECC gain is very high [30]. Very few LCCs open at such low voltage; however, since the membrane potential is so much lower than the Ca^{2+} Nernst potential, LCC unitary current is large, thus RyRs in the vicinity of an open LCC are more likely to open (RyR activation increases with $[Ca]_{dyad}$), thus resulting in RyR regenerative release and large ECC gain. At depolarized potentials, greater numbers of LCCs open, however the reduced unitary current has a lower probability of triggering RyR regenerative release. Thus, ECC gain decreases as membrane potential increases.

Simulation results from this study suggest that CaMKII phosphorylation modifies the ECC gain curve. In their experiments on rat ventricular myocytes, duBell et al [39] showed that exposure to increased amounts of PP1 and PP2A results in decreased ECC gain. This indicates that increased phosphorylation of ECC proteins results in increased gain. PP1 and PP2A target numerous proteins, including CaMKII, LCCs and RyRs, therefore making it difficult to infer the mechanism by which the phosphatases modulate gain. Nevertheless, assuming that increased phosphatase levels result in decreased LCC and RyR phosphorylation by CaMKII, Fig. 2 shows that the model is able to reproduce the qualitative features of the experimental results at positive potentials. The gain shifts reported from simulations are subtle compared to those presented in experiments. It is likely that other proteins are also responsible for shifts in ECC gain.

Model Assumptions and Limitations

A number of assumptions are made in the model. As in Greenstein and Winslow [16], it is assumed that there are 20 RyRs and 4 LCCs per CaRU. The number of RyRs modeled within each CaRU is quite conservative compared to the measurements recorded by Franzini-Armstrong et al [40], however it is close to the values recently observed by Hayashi et al [41] using 3D electron microscopy. If the CaRUs were modeled with a greater number of LCCs and RyRs in close proximity to each other, then it is possible that there would be even more RyR regenerative release and that diastolic leak and ECC gain would increase [42]. Despite these limitations, normalized simulated CaSpF displays a bell-shaped dependence on voltage, as seen in experiments [43] (see Figure DS2G).

A limitation of the model is that it is unable to replicate delayed after depolarizations (DADs), which are linked with CaMKII overexpression [37]. Generation of a DAD requires a large scale spontaneous Ca^{2+} release event to drive sufficient Na^{+}- Ca^{2+} exchanger current to underlie sufficient membrane depolarization. In this model, increased Ca_{SR} load will increase both the amplitude and frequency of resting Ca^{2+} sparks. However, since there is no detailed spatial tracking of Ca^{2+} concentration within the cell (i.e. no possibility of Ca waves), the model lacks the necessary mechanism by which spontaneous release events can rapidly trigger release from adjacent release sites in the absence of LCC triggers. Therefore, spontaneous synchronized large scale Ca^{2+} release events, and hence DADs, due not occur in this model.

The Shannon model was chosen over other RyR representations because it reproduces Ca^{2+} spark properties well, and it accounts for the role of $[Ca_{SR}]$ in RyR gating. It is a phenomenological representation of RyR gating, since the mechanisms underlying RyR inactivation are still not well understood. Early experiments show that increased $[Ca_{cyt}]$ results in decreased RyR open probability [44–47], while more recent studies have indicated that $[Ca_{JSR}]$ plays a more important role in termination of SR Ca^{2+} release [27,48–50]. As new data emerge, it will become possible to formulate better mechanistically based RyR models, and further improve understanding of CICR.

Final Thoughts and Predictions

In this study, it is assumed that CaMKII phosphorylation results in increased RyR sensitivity to Ca^{2+}. Interestingly it appears that under physiological conditions, this increase in sensitivity has only a minor impact on function. While there has been a great deal of interest in RyR phosphorylation and HF, the results from this study predict that attention should also be paid to the RyRs' neighbors across the dyad, the LCCs. Direct inhibition of LCC phosphorylation by CaMKII reduces mode 2 gating and diastolic RyR flux. Such inhibition may be the real key to reducing diastolic SR Ca^{2+} leak.

Supplementary Material

Refer to Web version on PubMed Central for supplementary material.

Acknowledgments

This work was supported by National Institutes of Health Grants R33HL87345 and PO1HL081427.

References

1. Hasenfuss G, Reinecke H, Studer R, Meyer M, Pieske B, Holtz J, et al. Relation between myocardial function and expression of sarcoplasmic reticulum Ca(2+)-ATPase in failing and nonfailing human myocardium. Circ Res 1994 September 1;75(3):434–442. 1994. [PubMed: 8062417]

2. O'Rourke B, Kass DA, Tomaselli GF, Kaab S, Tunin R, Marban E. Mechanisms of Altered Excitation-Contraction Coupling in Canine Tachycardia-Induced Heart Failure, I : Experimental Studies. Circ Res 1999 March 19;84(5):562–570. 1999. [PubMed: 10082478]

3. Ai X, Curran JW, Shannon TR, Bers DM, Pogwizd SM. Ca2+/Calmodulin-Dependent Protein Kinase Modulates Cardiac Ryanodine Receptor Phosphorylation and Sarcoplasmic Reticulum Ca2+ Leak in Heart Failure. Circ Res 2005 December 9;97(12):1314–1322. 2005. [PubMed: 16269653]

4. Marx SO, Reiken S, Hisamatsu Y, Jayaraman T, Burkhoff D, Rosemblit N, et al. PKA Phosphorylation Dissociates FKBP12.6 from the Calcium Release Channel (Ryanodine Receptor): Defective Regulation in Failing Hearts. Cell 2000;101(4):365–376. [PubMed: 10830164]

5. Shannon TR, Pogwizd SM, Bers DM. Elevated Sarcoplasmic Reticulum Ca2+ Leak in Intact Ventricular Myocytes From Rabbits in Heart Failure. Circ Res 2003 October 3;93(7):592–594. 2003. [PubMed: 12946948]

6. Kohlhaas M, Zhang T, Seidler T, Zibrova D, Dybkova N, Steen A, et al. Increased Sarcoplasmic Reticulum Calcium Leak but Unaltered Contractility by Acute CaMKII Overexpression in Isolated Rabbit Cardiac Myocytes. Circ Res 2006 February 3;98(2):235–244. 2006. [PubMed: 16373600]

7. Grandi E, Puglisi JL, Wagner S, Maier LS, Severi S, Bers DM. Simulation of Ca-Calmodulin-Dependent Protein Kinase II on Rabbit Ventricular Myocyte Ion Currents and Action Potentials. Biophys J 2007 December 1;93(11):3835–3847. 2007. [PubMed: 17704163]

8. Hashambhoy YL, Winslow RL, Greenstein JL. CaMKII-Induced Shift in Modal Gating Explains L-Type Ca2+ Current Facilitation: A Modeling Study. Biophysical Journal 2009;96(5):1770–1785. [PubMed: 19254537]

9. Hund TJ, Rudy Y. Rate Dependence and Regulation of Action Potential and Calcium Transient in a Canine Cardiac Ventricular Cell Model. Circulation 2004 November 16;110(20):3168–3174. 2004. [PubMed: 15505083]

10. Saucerman JJ, Bers DM. Calmodulin Mediates Differential Sensitivity of CaMKII and Calcineurin to Local Ca2+ in Cardiac Myocytes 2008;95(10):4597–4612.

11. Witcher DR, Kovacs RJ, Schulman H, Cefali DC, Jones LR. Unique phosphorylation site on the cardiac ryanodine receptor regulates calcium channel activity. J Biol Chem 1991 June 15;266(17): 11144–11152. 1991. [PubMed: 1645727]

12. Guo T, Zhang T, Mestril R, Bers DM. Ca2+/Calmodulin-Dependent Protein Kinase II Phosphorylation of Ryanodine Receptor Does Affect Calcium Sparks in Mouse Ventricular Myocytes. Circ Res 2006 August 18;99(4):398–406. 2006. [PubMed: 16840718]

13. Hain J, Onoue H, Mayrleitner M, Fleischer S, Schindler H. Phosphorylation Modulates the Function of the Calcium Release Channel of Sarcoplasmic Reticulum from Cardiac Muscle. J Biol Chem 1995 February 3;270(5):2074–2081. 1995. [PubMed: 7836435]

14. Lokuta AJ, Rogers TB, Lederer WJ, Valdivia HH. Modulation of cardiac ryanodine receptors of swine and rabbit by a phosphorylation-dephosphorylation mechanism. J Physiol 1995 September 15;487 (Pt_3):609–622. 1995. [PubMed: 8544125]

15. Yang D, Zhu W-Z, Xiao B, Brochet DXP, Chen SRW, Lakatta EG, et al. Ca2+/Calmodulin Kinase II-Dependent Phosphorylation of Ryanodine Receptors Suppresses Ca2+ Sparks and Ca2+ Waves in Cardiac Myocytes. Circ Res 2007 February 16;100(3):399–407. 2007. [PubMed: 17234969]

16. Greenstein JL, Winslow RL. An Integrative Model of the Cardiac Ventricular Myocyte Incorporating Local Control of Ca2+ Release. Biophys J 2002 December 1;83(6):2918–2945. 2002. [PubMed: 12496068]

17. Dzhura I, Wu Y, Colbran RJ, Balser JR, Anderson ME. Calmodulin kinase determines calcium-dependent facilitation of L-type calcium channels. Nat Cell Biol 2000;2(3):173–177. [PubMed: 10707089]

18. Erxleben C, Liao Y, Gentile S, Chin D, Gomez-Alegria C, Mori Y, et al. Cyclosporin and Timothy syndrome increase mode 2 gating of CaV1.2 calcium channels through aberrant phosphorylation of S6 helices. Proceedings of the National Academy of Sciences 2006 March 7;103(10):3932–3937. 2006.

19. Shannon TR, Wang F, Puglisi J, Weber C, Bers DM. A Mathematical Treatment of Integrated Ca Dynamics within the Ventricular Myocyte. Biophysical Journal 2004;87(5):3351–3371. [PubMed: 15347581]

20. Huke S, Bers DM. Ryanodine receptor phosphorylation at Serine 2030, 2808 and 2814 in rat cardiomyocytes. Biochemical and Biophysical Research Communications 2008;376(1):80–85. [PubMed: 18755143]
21. Wehrens XHT, Lehnart SE, Reiken SR, Marks AR. Ca2+/Calmodulin-Dependent Protein Kinase II Phosphorylation Regulates the Cardiac Ryanodine Receptor. Circ Res 2004 April 2;94(6):e61–e70. 2004. [PubMed: 15016728]
22. Huke S, Bers DM. Temporal dissociation of frequency-dependent acceleration of relaxation and protein phosphorylation by CaMKII. Journal of Molecular and Cellular Cardiology 2007;42(3):590–599. [PubMed: 17239900]
23. Hicks MJ, Shigekawa M, Katz AM. Mechanism by which cyclic adenosine 3':5'-monophosphate-dependent protein kinase stimulates calcium transport in cardiac sarcoplasmic reticulum. Circ Res 1979 March 1;44(3):384–391. 1979. [PubMed: 216505]
24. Shannon TR, Ginsburg KS, Bers DM. Reverse Mode of the Sarcoplasmic Reticulum Calcium Pump and Load-Dependent Cytosolic Calcium Decline in Voltage-Clamped Cardiac Ventricular Myocytes. Biophysical Journal 2000;78(1):322–333. [PubMed: 10620296]
25. Gupta RC, Kranias EG. Purification and characterization of a calcium-calmodulin-dependent phospholamban kinase from canine myocardium. Biochemistry 1989;28(14):5909–5916. [PubMed: 2775741]
26. Macdougall LK, Jones LR, Cohen P. Identification of the major protein phosphatases in mammalian cardiac muscle which dephosphorylate phospholamban. European Journal of Biochemistry 1991;196(3):725–734. [PubMed: 1849481]
27. Zima AV, Picht E, Bers DM, Blatter LA. Termination of Cardiac Ca2+ Sparks: Role of Intra-SR [Ca2+], Release Flux, and Intra-SR Ca2+ Diffusion. Circ Res 2008 October 10;103(8):e105–e115. 2008. [PubMed: 18787194]
28. Sobie EA, Guatimosim S, Gómez-Viquez L, Song L-S, Hartmann H, Saleet Jafri M, et al. The Ca2+ leak paradox and "rogue ryanodine receptors": SR Ca2+ efflux theory and practice. Progress in Biophysics and Molecular Biology 2005;90(1–3):172–185. [PubMed: 16326215]
29. Shannon TR, Ginsburg KS, Bers DM. Quantitative Assessment of the SR Ca2+ Leak-Load Relationship. Circ Res 2002 October 4;91(7):594–600. 2002. [PubMed: 12364387]
30. Wier WG, Egan TM, LÃ3pezez-LÃ3pez JR, Balke CW. Local control of excitation-contraction coupling in rat heart cells. The Journal of Physiology 1994 February 1;474(3):463–471. 1994. [PubMed: 8014907]
31. Hoch B, Meyer R, Hetzer R, Krause E-G, Karczewski P. Identification and Expression of {delta}-Isoforms of the Multifunctional Ca2+/Calmodulin-Dependent Protein Kinase in Failing and Nonfailing Human Myocardium. Circ Res 1999 April 2;84(6):713–721. 1999. [PubMed: 10189359]
32. Kirchhefer U, Schmitz W, Scholz H, Neumann J. Activity of cAMP-dependent protein kinase and Ca2+/calmodulin-dependent protein kinase in failing and nonfailing human hearts. Cardiovasc Res 1999 April 1;42(1):254–261. 1999. [PubMed: 10435018]
33. Tanskanen AJ, Greenstein JL, O'Rourke B, Winslow RL. The Role of Stochastic and Modal Gating of Cardiac L-Type Ca2+ Channels on Early After-Depolarizations. Biophys J 2005 January 1;88(1):85–95. 2005. [PubMed: 15501946]
34. Trafford AW, Dieaz ME, Eisner DA. Stimulation of Ca-induced Ca release only transiently increases the systolic Ca transient: measurements of Ca fluxes and sarcoplasmic reticulum Ca. Cardiovasc Res 1998 March 1;37(3):710–717. 1998. [PubMed: 9659455]
35. Curran J, Hinton MJ, Rios E, Bers DM, Shannon TR. {beta}-Adrenergic Enhancement of Sarcoplasmic Reticulum Calcium Leak in Cardiac Myocytes Is Mediated by Calcium/Calmodulin-Dependent Protein Kinase. Circ Res 2007 February 16;100(3):391–398. 2007. [PubMed: 17234966]
36. Anderson ME, Braun AP, Wu Y, Lu T, Wu Y, Schulman H, et al. KN-93, an Inhibitor of Multifunctional Ca++/Calmodulin-Dependent Protein Kinase, Decreases Early Afterdepolarizations in Rabbit Heart. J Pharmacol Exp Ther 1998 December 1;287(3):996–1006. 1998. [PubMed: 9864285]
37. Sag CM, Wadsack DP, Khabbazzadeh S, Abesser M, Grefe C, Neumann K, et al. Calcium/Calmodulin-Dependent Protein Kinase II Contributes to Cardiac Arrhythmogenesis in Heart Failure. Circ Heart Fail 2009 November 1;2(6):664–675. 2009. [PubMed: 19919992]

38. Venetucci LA, Trafford AW, Eisner DA. Increasing Ryanodine Receptor Open Probability Alone Does Not Produce Arrhythmogenic Calcium Waves: Threshold Sarcoplasmic Reticulum Calcium Content Is Required. Circ Res 2007 January 5;100(1):105–111. 2007. [PubMed: 17110597]

39. duBell WH, Lederer WJ, Rogers TB. Dynamic modulation of excitation-contraction coupling by protein phosphatases in rat ventricular myocytes. The Journal of Physiology 1996 June 15;493(Pt 3): 793–800. 1996. [PubMed: 8799900]

40. Franzini-Armstrong C, Protasi F, Ramesh V. Shape, Size, and Distribution of Ca2+ Release Units and Couplons in Skeletal and Cardiac Muscles. Biophysical Journal 1999;77(3):1528–1539. [PubMed: 10465763]

41. Hayashi T, Martone ME, Yu Z, Thor A, Doi M, Holst MJ, et al. Three-dimensional electron microscopy reveals new details of membrane systems for Ca2+ signaling in the heart. J Cell Sci 2009 April 1;122(7):1005–1013. 2009. [PubMed: 19295127]

42. Greenstein JL, Hinch R, Winslow RL. Mechanisms of Excitation-Contraction Coupling in an Integrative Model of the Cardiac Ventricular Myocyte. Biophys J 2006 January 1;90(1):77–91. 2006. [PubMed: 16214852]

43. Santana LF, Cheng H, Gomez AM, Cannell MB, Lederer WJ. Relation Between the Sarcolemmal Ca2+ Current and Ca2+ Sparks and Local Control Theories for Cardiac Excitation-Contraction Coupling. Circ Res 1996 January 1;78(1):166–171. 1996. [PubMed: 8603501]

44. Chamberlain BK, Volpe P, Fleischer S. Calcium-induced calcium release from purified cardiac sarcoplasmic reticulum vesicles. General characteristics. Journal of Biological Chemistry 1984 June 25;259(12):7540–7546. 1984. [PubMed: 6736018]

45. Fabiato A. Time and calcium dependence of activation and inactivation of calcium-induced release of calcium from the sarcoplasmic reticulum of a skinned canine cardiac Purkinje cell. J Gen Physiol 1985 Feb;85(2):247–289. [PubMed: 2580043]

46. ZimÃ¡nyi I, Pessah IN. Comparison of [3H]ryanodine receptors and Ca++ release from rat cardiac and rabbit skeletal muscle sarcoplasmic reticulum. Journal of Pharmacology and Experimental Therapeutics. 1991 1991 March;256(3):938–946.

47. Gyorke I, Gyorke S. Regulation of the cardiac ryanodine receptor channel by luminal Ca2+ involves luminal Ca2+ sensing sites. Biophys J 1998 Dec;75(6):2801–2810. [PubMed: 9826602]

48. Stevens SC, Terentyev D, Kalyanasundaram A, Periasamy M, Gyorke S. Intra-sarcoplasmic reticulum Ca2+ oscillations are driven by dynamic regulation of ryanodine receptor function by luminal Ca2+ in cardiomyocytes. J Physiol 2009 Oct 15;587(Pt 20):4863–4872. [PubMed: 19703963]

49. Terentyev D, Viatchenko-Karpinski S, Valdivia HH, Escobar AL, Gyorke S. Luminal Ca2+ Controls Termination and Refractory Behavior of Ca2+-Induced Ca2+ Release in Cardiac Myocytes. Circ Res 2002 September 6;91(5):414–420. 2002. [PubMed: 12215490]

50. Zima AV, Picht E, Bers DM, Blatter LA. Partial Inhibition of Sarcoplasmic Reticulum Ca Release Evokes Long-Lasting Ca Release Events in Ventricular Myocytes: Role of Luminal Ca in Termination of Ca Release. Biophysical Journal 2008;94(5):1867–1879. [PubMed: 18024505]

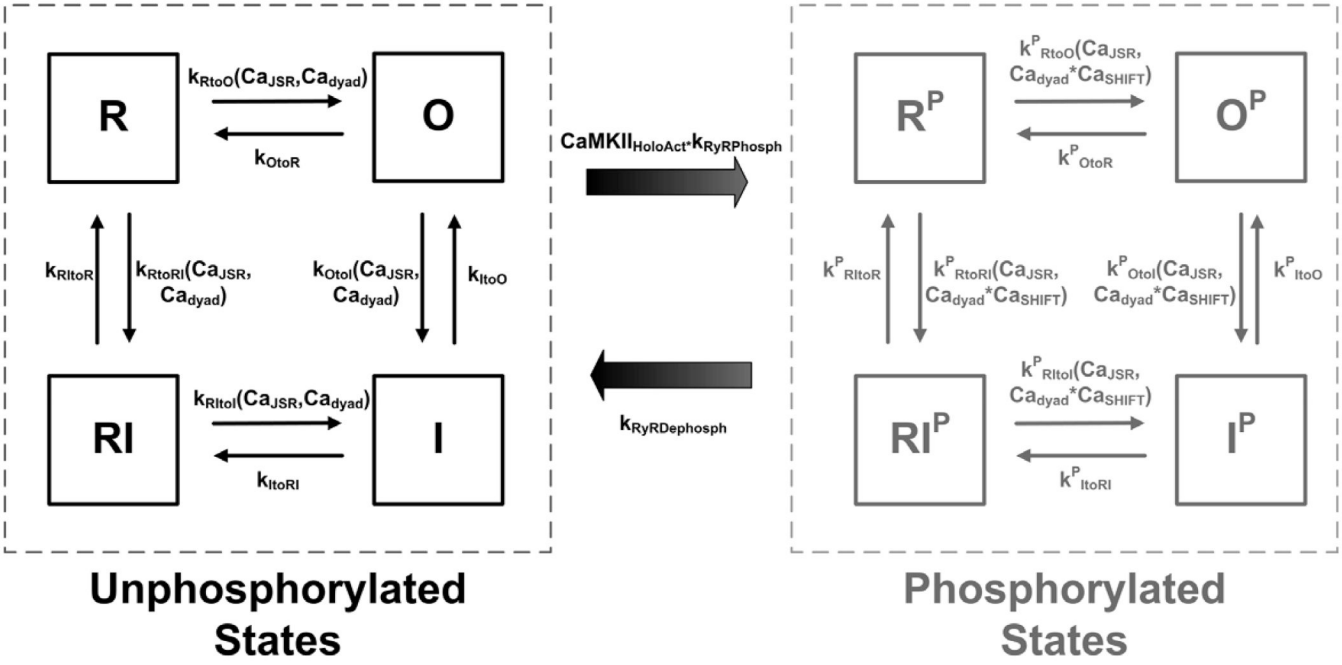

Figure 1.

RyRs state model. Unphosphorylated RyR states are on the left and phosphorylated states are on the right. Transition rates within each sub-group are a function of $[Ca_{dyad}]$ and $[Ca_{JSR}]$, similar to the dependence on $[Ca_{cyt}]$ and $[Ca_{SR}]$ in Shannon et al [19]. Phosphorylated RyRs have an increased affinity for Ca^{2+}, represented by the factor Ca_{Shift}. The phosphorylation rate is a function of local CaMKII activity.

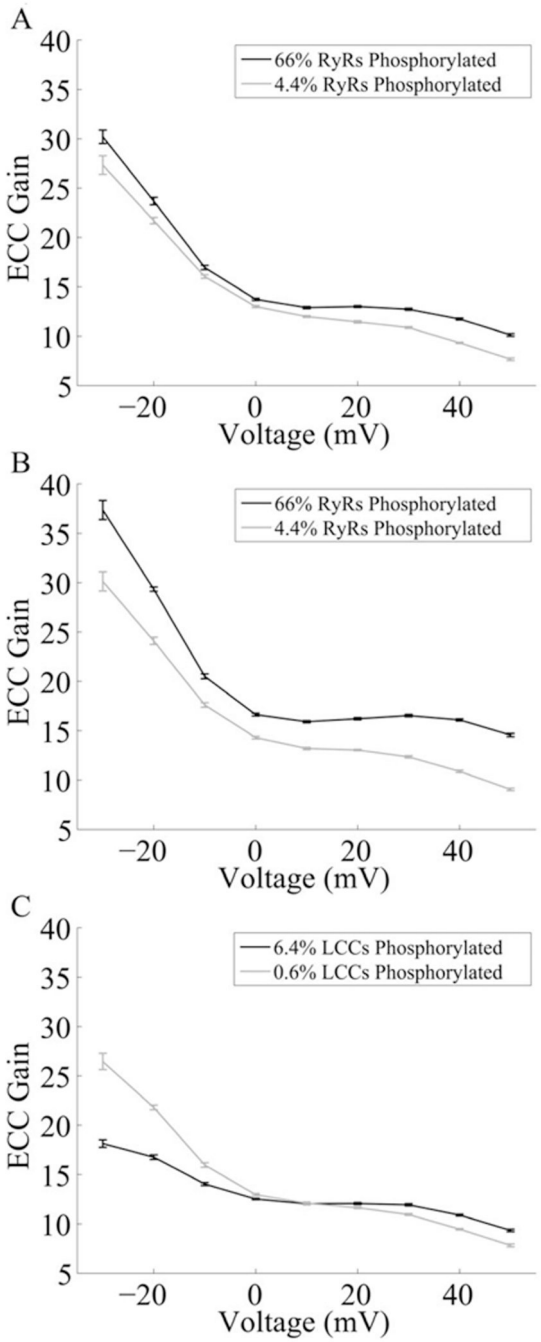

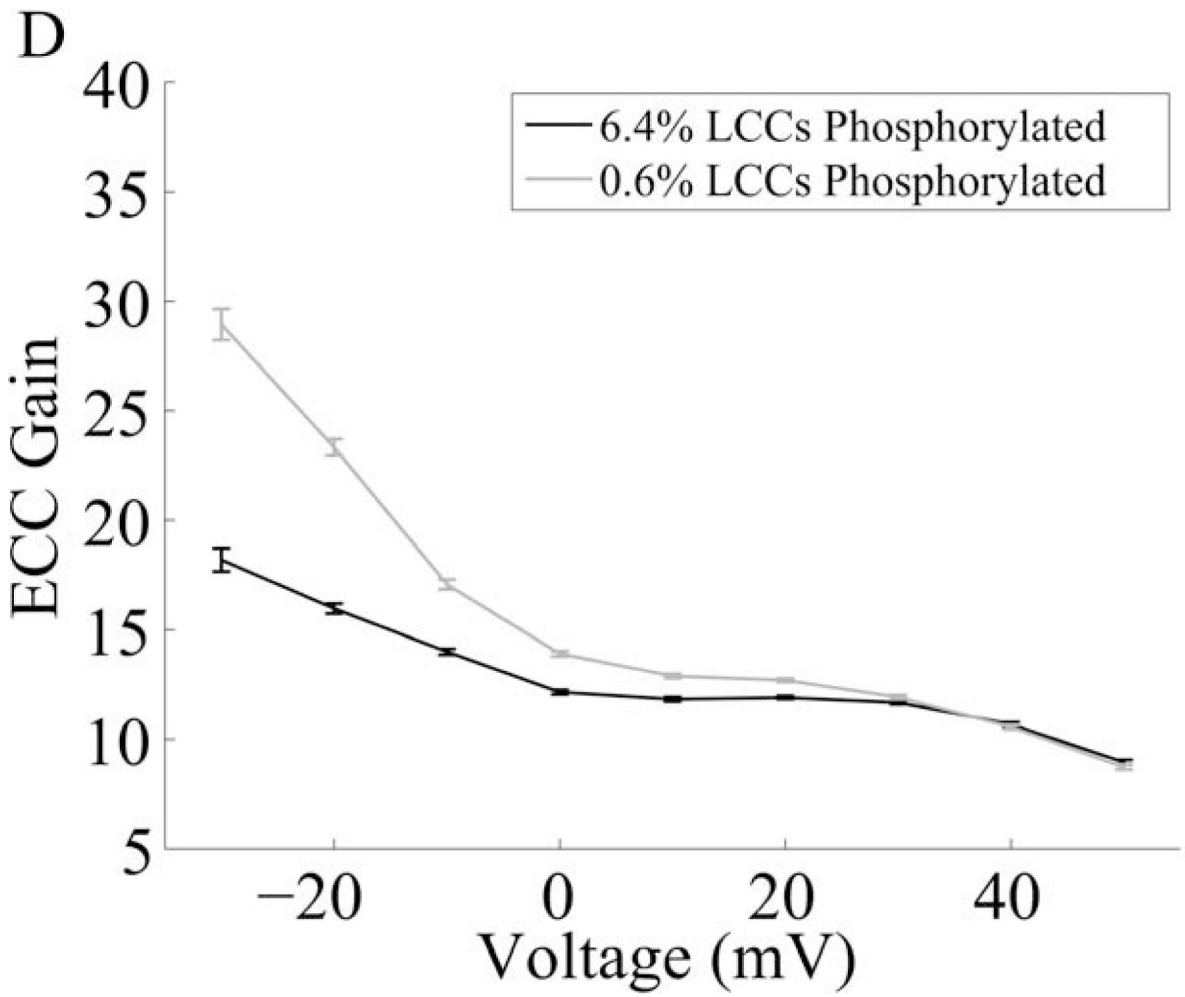

Figure 2.

Simulated ECC Gain under varying degrees of LCC and RyR phosphorylation. To load the SR with Ca^{2+}, membrane potential was clamped to 0 mV for 200 ms from a holding potential of −70 mV repeatedly at 0.5 Hz for 10 s. Membrane potential was then clamped to a variable test potential for 200 ms. ECC gain is calculated using peak LCC and RyR flux obtained during the test potential. The simulation was performed 20 times at each membrane potential. Results are presented as mean ± S.E.M. (A) ECC gain in the absence of LCC phosphorylation, with varying degree of RyR phosphorylation. The maximum RyR phosphorylation rate was altered to 25% or 1000% of normal to obtain 4.4% or 66% RyR phosphorylation, respectively. (B) Same protocol as panel A where prior to the test pulse, Ca_{SR} was set to 0.75 mM and Ca_{cyt} was set to 75 nM. (C) ECC gain in the absence of RyR phosphorylation, with varying degree of LCC phosphorylation. The maximum LCC phosphorylation rate was altered to 50% or 150% of normal to obtain 0.6% or 6.4% LCC phosphorylation, respectively. (D) Same protocol as panel C where prior to the test pulse, Ca_{SR} was set to 0.75 mM and Ca_{cyt} was set to 75 nM.

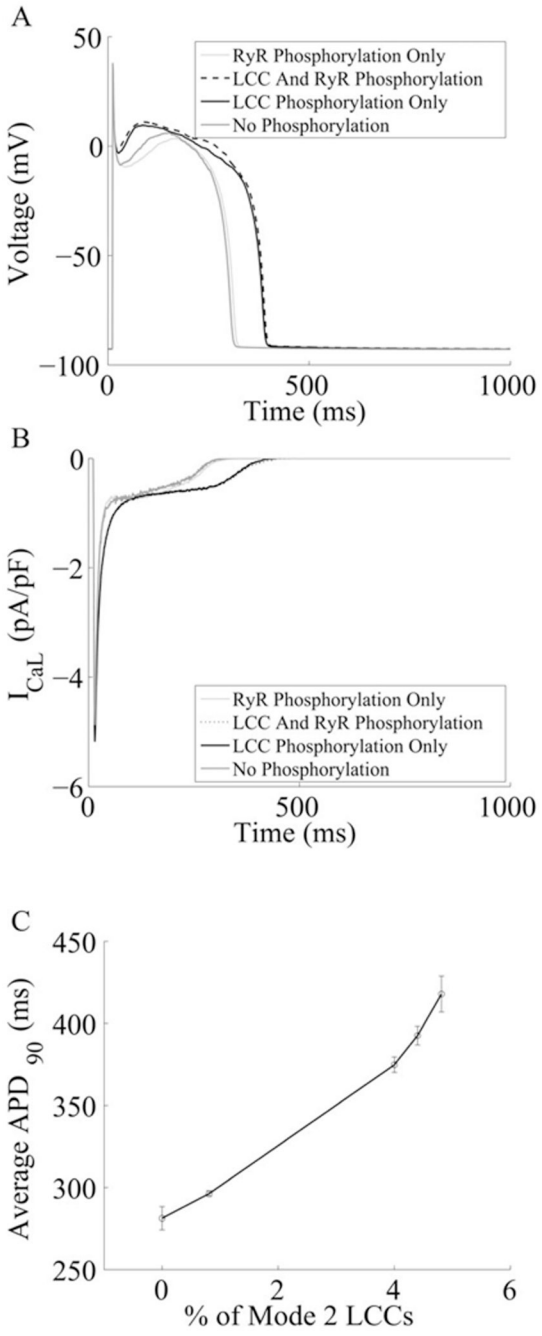

Figure 3.

Simulated Results from a 1Hz AP pacing protocol under different phosphorylation conditions. Every second, a current with −100 pA/pF amplitude and 0.5 ms duration is applied to the membrane to stimulate APs. For each condition, 50 s of pacing is simulated and the results from all 50 APs are averaged and presented. Average results are presented. (A) APs and (B) I_{CaL}. (C): APD as a function of average LCC phosphorylation levels.

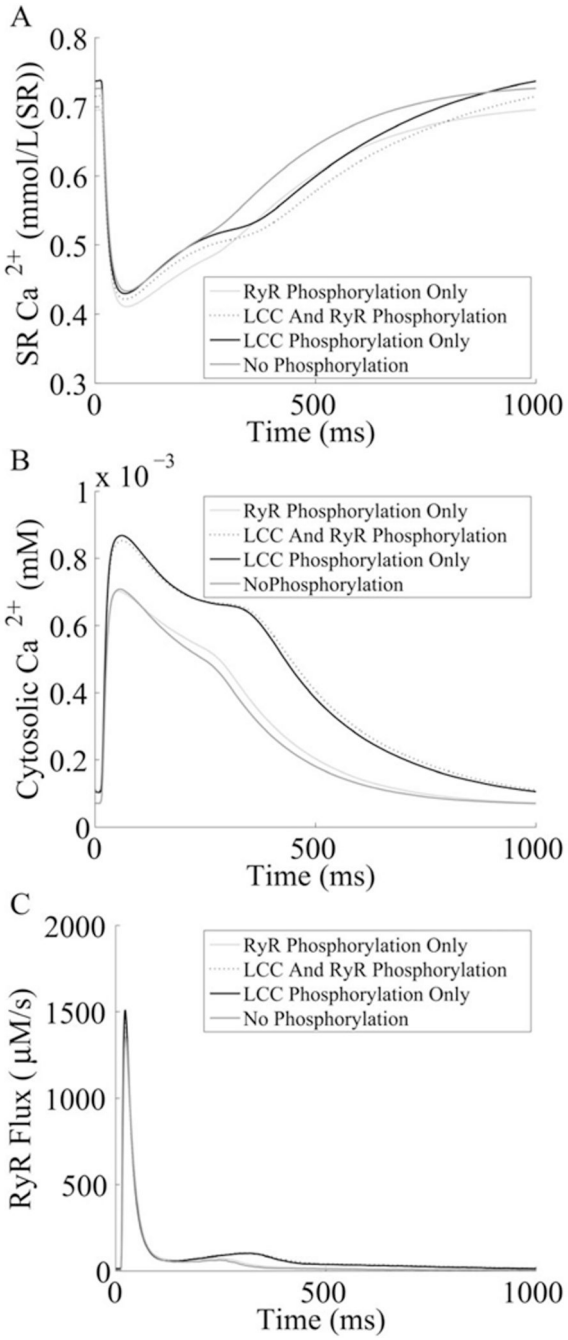

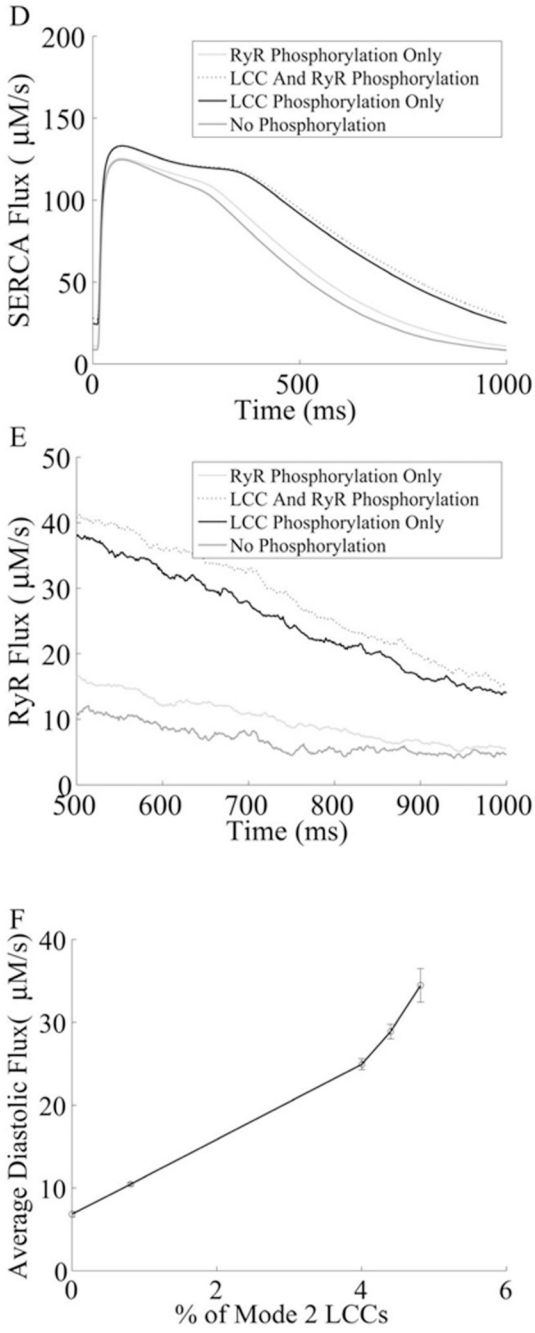

Figure 4.

Simulated Results of Ca^{2+} dynamics under a 1Hz AP pacing protocol under different phosphorylation conditions. The protocol is the same as in Fig. 3. (A) [Ca_{SR}] (mmol/L SR). (B) [Ca_{cyt}] (mmol/L cytosol) (C) RyR Flux (μmol/L cytosol/s). (D) SERCA flux, i.e., net Ca^{2+} pumped into the SR via SERCA (μmol/L cytosol/s). (E) Diastolic RyR Flux (zoomed in plot of (C)). (F) Average Diastolic RyR Flux at varying levels of LCC phosphorylation (these levels were modified by varying LCC phosphorylation rates).

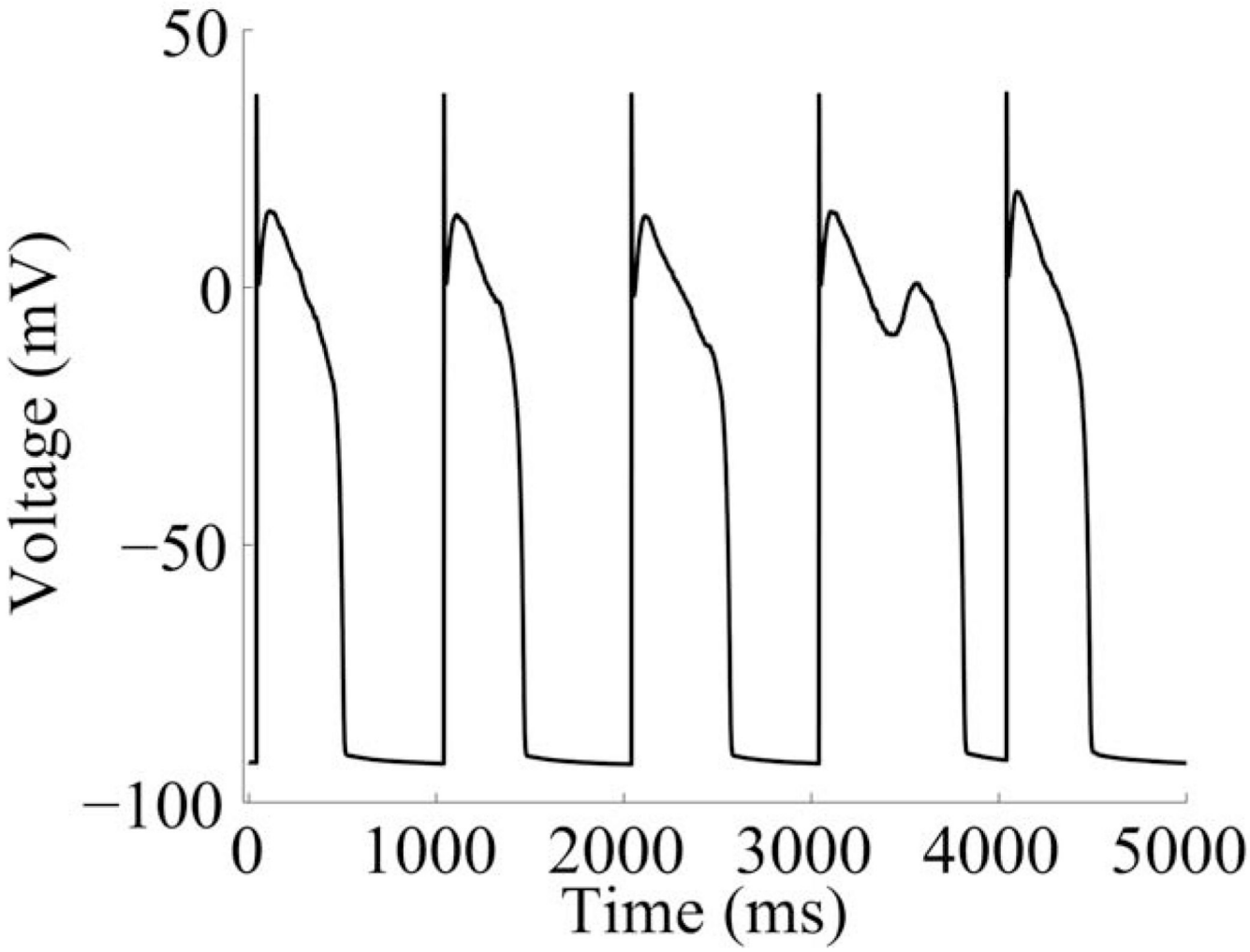

Figure 5.
A simulated EAD under a 1Hz pacing protocol where the LCC phosphorylation rate is increased by 10%.